Nonadiabatic superconductivity. I. Vertex corrections for the electron-phonon interactions

L. Pietronero
Dipartimento di Fisica, Università di Roma "La Sapienza," Piazzale Aldo Moro, 2, 00185 Roma, Italy

S. Strässler
HUBA Control AG Industriestrasse 17, CH-8116 Würenlos, Switzerland

C. Grimaldi
Max Planck Institut für Physik Komplexer Systeme, Aussenstelle Stuttgart, Heisenbergstrasse 1, 70569 Stuttgart, Germany
(Received 1 June 1994; revised manuscript received 8 December 1994)

High-temperature superconductors, including the fullerene compounds, are all characterized by a very small value of the Fermi energy (E_F), of the order of the Debye phonon frequency (ω_D). This implies a breakdown of Migdal's theorem for the electron-phonon interactions and it requires a generalization of the many-body theory of superconductivity. In this and in the following paper we consider the first steps of this generalization in a perturbative scheme with respect to the parameter ($\lambda\omega_D/E_F$). Here we discuss in detail the vertex correction function and the self-energy for $\omega_D/E_F \neq 0$. The main result is that the vertex function shows a complex behavior with respect to the momentum (q) and frequency (ω) of the exchanged phonon. In particular vertex corrections are positive for small values of q. We discuss that the small q region may be favored by electronic correlations and by density of states effects. In such a situation it is possible to obtain a strong enhancement of T_c with respect to the usual theory. In addition vertex corrections and other effects due to the breakdown of Migdal's theorem should have important consequences on other properties like the isotope effect, transport properties, phonon frequencies, tunneling and photoemission data. The essential results of this and the next paper should also apply to cases in which the attractive interaction of the electron pairs is due to a bosonic excitation different from phonons.

I. INTRODUCTION

All high-T_c superconductors are characterized by a very small value of the Fermi energy E_F. From the data of Ref. 1, confirmed by various other experiments, one obtains $E_F \simeq 0.1-0.3$ eV for oxide superconductors. A_3C_{60} compounds, chevrel phases and organic superconductors. The Debye phonon frequencies ω_D range from 80 meV for the oxides to 160 meV for the fullerene compounds. This situation implies a breakdown of Migdal's theorem[2,3] because the ratio ω_D/E_F is not negligible and the energies of electrons and phonons are comparable. Migdal's theorem corresponds to an adiabatic approximation for the dynamics of electrons and phonons and it allows one to neglect vertex corrections and other effects in dealing with the electron-phonon interactions. Within such an approximation it is possible to generalize the BCS theory of superconductivity to include all the many-body effects. This leads to the Eliashberg equations[4,5] for which the most popular expression for T_c is the McMillan one.[6] These many-body effects produce a strong reduction of T_c with respect to the BCS expression and are essential for the argument, shared by several authors, that electron-phonon superconductivity is limited by a maximum $T_c \approx 20-30$ K.[7] This argument, together with the evidence for strong electronic correlations in the oxides seemed to make the electron-phonon interaction as hopeless to explain the high-T_c materials and stimulated the search for radically new mechanisms.[8,9] The breakdown of Migdal's theorem however leads to a very different situation that we are going to study in this and in the following paper (paper II).[10]

Our point of view is the following: it is clear that the phase diagram of the cuprates or the properties of fullerene compounds as a function of the band filling[11] require to start from a Hubbard-type Hamiltonian or in any case from concepts more complex than the simple Fermi liquid. It is also the case however that superconductivity is always associated to a metallic behavior above T_c and that the phenomenology of the superconducting state is relatively normal, apart of course from the value of T_c and a few other properties. Also for the normal state various elements point to a Fermi-liquid phenomenology[12–14] even though important anomalies are present. Since we will refer only to these properties we will adopt the Fermi liquid as a starting concept. From this point of view the description of the superconducting compounds implies unavoidably the breakdown of Migdal's theorem.[15,16] In this and in the following paper we focus on this point and try to derive its implications as far as possible. This implies necessarily certain drastic simplifications with respect to other elements, like the Coulomb interactions, that are certainly important in these systems. We are going to see however that electronic correlations due to Coulomb interactions can play an important role also in the present framework by

enhancing the positive regions of the vertex corrections.

We have named this generalization of the theory of superconductivity as "nonadiabatic superconductivity." Clearly also the standard superconductivity is a nonadiabatic phenomenon and here we mean that, in addition, the electron-phonon coupling is also nonadiabatic. We believe however that this title is compact and unambiguous. After all, "high-T_c superconductivity" also refers to low-temperature phenomena.

In Sec. II, we present a simplified discussion of the self-energy effects on superconductivity and of the role played by vertex corrections. In particular, we show that it is consistent to discuss the breakdown of Migdal's theorem within a perturbative scheme. Within this scheme the high-T_c phenomenology that is now interpreted via Eliashberg equations in terms of very strong coupling ($\lambda \simeq 3$) can be reinterpreted, in case of positive vertex corrections, from a weak-coupling scheme with $\lambda \simeq 0.5-1.0$.

In Sec. III we define the specific model assumptions that we are going to use here and in paper II and recompute the usual self-energy in the case $\omega_D/E_F \neq 0$. The result corresponds to a reduction of the wave-function renormalization term and therefore to an enhancement of T_c.

In Sec. IV, we present an analytical calculation of the vertex correction function including explicitly the dependence on the momentum (q) and frequency (ω) of the exchanged phonon. The structure of this function is quite complex and even its sign depends explicitly on q and ω. In particular, positive values are obtained for small values of q.

In Sec. V, we discuss the role of specific material properties. In particular, we present simple arguments that indicate that electronic correlations may favor positive vertex corrections and contribute therefore to an enhancement of T_c. Also the problem of the pseudopotential μ^* is briefly discussed.

In Sec. VI, we show how the simplified picture of Sec. II is supported by a more detailed analysis and discuss a simplified equation for T_c. The breakdown of Migdal's theorem is expected to have important consequences for the isotope effect and various other properties.

II. SIMPLIFIED DESCRIPTION OF MANY-BODY EFFECTS AND VERTEX CORRECTIONS

In this section we present some arguments that allow one to construct a simple, intuitive picture, of the role of electron-phonon many-body effects in superconductivity. The following sections and paper II will provide a more systematic treatment that is however going to confirm the essence of the simple picture we expose here.

We start by showing how self-energy effects within Migdal's theorem modify the BCS equation for T_c into the McMillan expression and then we consider also the inclusions of vertex corrections. Starting from the BCS expression for T_c (including the Coulomb term μ^*)

$$T_c \cong \langle \omega \rangle e^{-1/(\lambda-\mu^*)} \tag{2.1}$$

as arising from the usual scattering diagram of Fig. 1(a).

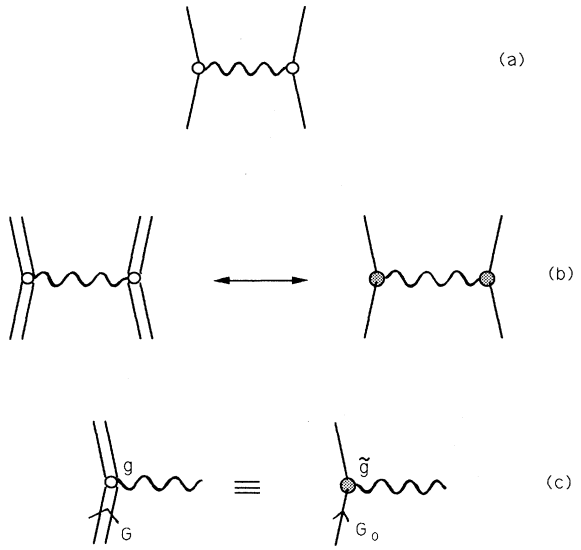

FIG. 1. (a) Standard BCS diagram; (b) the effect of electron-self-energy in the dressed Green's function (double lines) is absorbed in the definition of an effective vertex; (c) the effective vertex corresponds to the bare one divided by the Z of the incoming electron propagator.

Then we would like to modify this expression to include self-energy effects [Fig. 1(b), left] without going through the usual Eliashberg discussion. Our basic idea will be to absorb the effect of electron self-energy in the definition of a new effective coupling $\tilde{\lambda}$ [Fig. 1(b)]. Note that this has nothing to do with the vertex corrections that we will consider later.

Considering the real part of the self-energy, the electron propagator is[3]

$$G(\mathbf{k},\omega)=\frac{1}{\omega-\varepsilon_k-\Sigma(\mathbf{k},\omega)} . \tag{2.2}$$

By expanding as usual

$$\Sigma(k,\omega)=\Sigma(0)+\frac{\partial\Sigma}{\partial\omega}(\omega) , \tag{2.3}$$

one defines the coupling

$$\lambda=-\frac{\partial\Sigma}{\partial\omega} \tag{2.4}$$

and the wave-function renormalization term

$$Z=1-\frac{\partial\Sigma}{\partial\omega}=(1+\lambda) . \tag{2.5}$$

The propagator [Eq. (2.2)] can be rewritten as

$$G(\mathbf{k},\omega)=\frac{1}{Z}\frac{1}{\omega-\varepsilon_k/Z} . \tag{2.6}$$

The self-energy therefore has two effects: the first one is to renormalize the band dispersion near the Fermi level. This enhances the density of states (DOS) because the Fermi velocity is reduced[5]

$$\tilde{N}(0)=N(0)(1+\lambda) \tag{2.7}$$

and it also enhances the effective mass

$$m^*=m(1+\lambda) . \tag{2.8}$$

The second effect is to reduce the spectral weight of the coherent part of the propagator. It is possible to absorb the prefactor $1/Z$ into an effective vertex in order to deal with propagators that do not contain the wave-function renormalization prefactor. This concept is illustrated in Fig. 1(c) and it corresponds to writing

$$g_{k,k'}G(k,\omega)=\left[g_{k,k'}\frac{1}{Z}\right]G_0(k,\omega) , \tag{2.9}$$

where G_0 represents the bare propagator with a renormalized dispersion.

In practice every double line (G) ending into a vertex g is substituted by a single line (G_0) with a modified vertex [Figs. 1(b) and 1(c)]:

$$\tilde{g}=g\frac{1}{Z} . \tag{2.10}$$

We can now use the BCS expression (2.1), referring to the new G_0 (with modified DOS) and with a vertex $\tilde{g}$. This leads to an effective coupling

$$\tilde{\lambda}=\tilde{g}^2\tilde{N}(0)=\frac{\lambda}{1+\lambda} \tag{2.11}$$

that, inserted into Eq. (2.1) instead of the original λ, gives

$$T_c\cong\langle\omega\rangle e^{-(1+\lambda)/[\lambda-\mu^*(1+\lambda)]} \tag{2.12}$$

that is quite close to the McMillan expression.[6] Looking at Eq. (2.11) we can make a simple interpretation of the effects of self-energy. The density of states is enhanced by a factor $(1+\lambda)$ but the coupling (g^2) is reduced by $(1+\lambda)^2$ so the total effect is a reduction by a factor $(1+\lambda)$. This term is responsible for the reduction of T_c from the BCS to the McMillan formula. We see therefore that, within Migdal's theorem many body effects suppress the value of T_c.

At this level of discussion it is easy to introduce also the effect of vertex corrections (Fig. 2). Migdal's theorem states that, if a bare vertex has an amplitude g, the correction is of the order $g[\lambda(\omega_D/E_F)]$.[2,3] Therefore if $\omega_D/E_F\to 0$ these corrections are negligible even if λ is large. Considering instead the situation in which ω_D/E_F is not zero but rather of the order of unity we have a more complex situation. In order to clarify these effects it is useful to consider the addition of a phonon line to the basic BCS diagram (Fig. 3). If the phonon is added in position (a) this corresponds to a self-energy effect and it gives a contribution of the order of λ as we have seen in Eq. (2.11). If instead we add the phonon in the position (b) this corresponds to a vertex correction and the contribution is of the order $\lambda(\omega_D/E_F)$. Migdal's theorem allows one to disregard this diagram in view of the term ω_D/E_F but not because it is of higher order in λ. The effects of the breakdown of Migdal's theorem therefore can be studied in a perturbative scheme. For example, if $\omega_D/E_F\approx 1$ and $\lambda<1$ Migdal's theorem does not hold but the two contributions [Figs. 3(a) and 3(b)] are of the same order and both relatively small. This clarifies also that the breakdown of Migdal's theorem can coexist with a Fermi-liquid picture. Of course this may imply some nontrivial deviations from the ideal Fermi-liquid picture, nevertheless a perturbative scheme based on propagating electrons preserves its validity.

We consider now the addition of vertex corrections to the many-body effects discussed before. In this case the bare vertex g should be substituted by (Fig. 2)

$$g'=g\left[1+\lambda\frac{\omega_D}{E_F}p(q,\omega)+\cdots\right] , \tag{2.13}$$

where the function $p(q,\omega)$ characterizes the dependence of the vertex corrections on the frequency and momentum of the outgoing phonon (q,ω). We are going to see in the fourth section that the momentum and frequency dependence of the vertex function is quite complex and it can be positive or negative. One should then consider the role of this function on the gap equation. In order to study its main effect on the transition temperature we can consider an effective average $\langle p(q,\omega)\rangle$ that also can be positive or negative depending on the details of the problem. In a favorable situation (see fourth section and paper II) we can assume that $\langle p(q,\omega)\rangle\simeq 1$. In the case $\omega_D/E_F\simeq 1$ we can then use Eq. (2.13) into (2.11) and obtain the new effective coupling

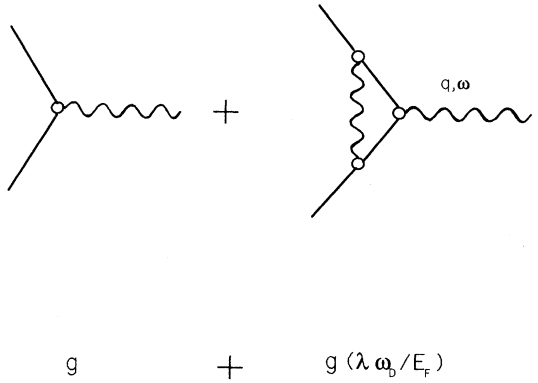

FIG. 2. Bare vertex and first-order vertex corrections for electron-phonon scattering.

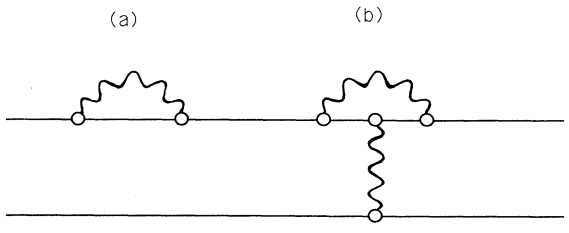

FIG. 3. The addition of a phonon line in position (a) to the standard BCS diagram corresponds to a self-energy effect and it gives a contribution of order λ. The addition of a phonon line in position (b) corresponds instead to a vertex correction and is of order $\lambda\omega_D/E_F$.

$$\tilde{\lambda}=\frac{\lambda[1+\lambda(\omega_D/E_F)\langle p(q,\omega)\rangle]^2}{(1+\lambda)}\cong\lambda(1+\lambda)\ . \quad (2.14)$$

This leads then to a rather different expression for T_c (Ref. 13) with respect to Eq. (2.12):

$$T_c\cong\langle\omega\rangle e^{-1/[\lambda(1+\lambda)-\mu^*]}\ . \quad (2.15)$$

This discussion is highly simplified and we are going to see in the following how to make it more systematic. However it is useful to clarify the main effects of vertex corrections in a favorable situation.

Consider, for example, the comparison between the graphite intercalation compounds KC_8 and fullerene compounds (A_3C_{60}) as shown in Table I. This comparison is particularly relevant because the two systems have strong similarities in the electronic and vibrational properties. Therefore, even if there may be an appreciable indetermination in the absolute values of the parameters (say λ), the relative difference is much more meaningful. In this respect it would by very useful if microscopic calculations of λ for A_3C_{60} would be accompanied by analogous calculations for KC_8.

The transition temperatures differ by more than 2 orders of magnitude and even if λ can be somewhat larger for the fullerene compounds, the larger value of μ^* (Ref. 26) actually compensates this advantage. Therefore from a standard Migdal-Eliashberg point of view, not only the fullerene compounds are far from ideal, but it is not even possible to understand why their T_c values should be larger than the very low T_c of graphite compounds.

If we consider the value of the Fermi energy of the two systems we can see however that the situation is completely different. Graphite compounds have a broad band with a Fermi energy of several eV. In such a case Migdal's theorem holds ($\omega_D/E_F\cong0.02$) and the small value of T_c is consistent with the McMillan expression. In the fullerene compounds the electronic states are instead distributed in many narrow bands. These bands are separated by gaps of about 2 eV, therefore the scattering with phonons is limited to the single band in which the Fermi level is located. This leads to $E_F\simeq0.2$ eV and it implies the breakdown of Migdal's theorem ($\omega_D/E_F\approx1$). Note that Coulomb scattering can instead extend over many bands and this is the reason for having a not too large value of μ^*. If the vertex corrections are mainly positive we can use instead Eq. (2.15) that gives a T_c value compatible with the parameters of the fullerene compounds.

TABLE I. In the estimation of superconductivity parameters the comparison of graphite intercalation compounds (KC_8) and fullerene compounds (A_3C_{60}) is particularly interesting because many properties are similar while the T_c values are very different. From the estimated parameters shown one can see that the KC_8 compound is well compatible with the usual theory [Eq. (2.12)]. On the contrary the A_3C_{60} compounds are far from ideal from a Migdal-Eliashberg point of view. Actually a basic difference between the two systems can be found in the value of the Fermi energy and in the fact that Migdal's theorem is strongly violated for A_3C_{60}. A review of the fullerene data can be found in Ref. 13, while the graphite data are from Ref. 33.

	KC_8	A_3C_{60}
T_c	0.1–0.2 K	20–35 K
ω_D	2000 K	2000 K
λ	~0.25	~0.5
μ^*	0.1	0.4
E_F	10 eV	0.2 eV

It is interesting to note that if one would use the value of T_c to determine λ via the McMillan equation, one would obtain an anomalously large value of λ. Our point is instead that the real value of λ is normal (0.5–1) but the equation should be changed. For example, a large amount of data for the oxide superconductors can be reproduced via the usual Eliashberg equations with $\lambda\simeq3$,[17] that is considered an unrealistic value. This implies that [Eq. (2.11)]

$$\tilde{\lambda}=\frac{\lambda}{1+\lambda}\cong0.75\ . \quad (2.16)$$

If vertex corrections are important we should instead use Eq. (2.14),

$$\tilde{\lambda}=\lambda(1+\lambda)\cong0.75\ , \quad (2.17)$$

that leads to the more realistic value $\lambda\approx0.5$. This is a very important point because it shows that the inclusion of vertex corrections even at a perturbative level may allow one to reinterpret data that according to the usual theory lead to anomalously large coupling ($\lambda\simeq3$) as arising instead from a situation of weak-intermediate coupling ($\lambda\simeq0.5$).

In the following sections and in paper II we are going to reconsider this whole matter in a more systematic way. However the main conclusions of this simplified discussion will be confirmed provided that the vertex corrections are mainly positive. We are going to see that this is the case if the small-q scattering is dominating or in other specific situations. It is interesting to note that the inclusion of electronic correlations in the problem actually produces a modulation of the electron-phonon scattering which favors the small momentum scattering. In our perspective therefore the main effect for the high-T_c phenomenon is in the breakdown of Migdal's theorem. However, electronic correlations should be also essential to bring the system in a range of favorable parameters with respect to the sign of the vertex corrections.

III. THE MODEL AND THE SELF-ENERGY

The model Hamiltonian is the usual one[16]

$$H=\sum_{\mathbf{k}}\varepsilon(\mathbf{k})c_{\mathbf{k}}^{\dagger}c_{\mathbf{k}}+\sum_{\mathbf{q}}\omega_0 b_{\mathbf{q}}^{\dagger}b_{\mathbf{q}}+\frac{g}{\sqrt{N}}\sum_{\mathbf{k},\mathbf{q}}c_{\mathbf{k}+\mathbf{q}}^{\dagger}c_{\mathbf{k}}(b_{\mathbf{q}}+b_{-\mathbf{q}}^{\dagger}) \quad (3.1)$$

corresponding to the coupling of a single Einstein mode with frequency ω_0 to an electronic band characterized by a dispersion $\varepsilon(k)$ and a chemical potential μ. In order to

perform analytical calculations we adopt a simplified scheme based on the following assumptions.

The density of states is assumed to be constant (N_0) between $-E/2$ and $E/2$ with a Fermi energy at zero. This corresponds to a half-filled band with $E_F=E/2$.

The q dependence is considered only for the scattering. For integrations over the Brillouin zone we use the simplification

$$x=\varepsilon(k)-\mu, \quad -\frac{E}{2}<x<\frac{E}{2} , \tag{3.2}$$

$$\sum_{\mathbf{k}} \rightarrow N_0 \int_{-E/2}^{E/2} dx . \tag{3.3}$$

In general one may have a coupling $g_{\mathbf{k},\mathbf{k}+\mathbf{q}}$ explicitly dependent on $\mathbf{k}$ and $\mathbf{q}$. Here we consider simply a constant value g. We are going to see however that the dependence on $\mathbf{q}$ maybe very important and this is a point that we will reconsider in the following and in paper II.

The dimensionless coupling is defined as usual

$$\lambda=g^2 N_0 . \tag{3.4}$$

Considering a parabolic dispersion

$$\varepsilon(\mathbf{k})=\frac{k^2}{2m}-\mu , \tag{3.5}$$

$$\varepsilon(\mathbf{k}-\mathbf{q})=\frac{k^2}{2m}+\frac{q^2}{2m}-\frac{\mathbf{q}\cdot\mathbf{k}}{m}\eta-\mu, \quad \eta=\cos\vartheta , \tag{3.6}$$

where ϑ is the scattering angle, we can identify

$$E=\frac{k_F^2}{m}, \quad \mu=\frac{k_F^2}{2m} . \tag{3.7}$$

At this stage we are going to neglect the q^2 term in Eq. (3.6), so our results hold for not too large values of q. Later however we will see that the inclusion of these quadratic terms does not change the results appreciably. In practice these approximations correspond to assuming a locally linear dispersion of the band in the vicinity of k_F:

$$\varepsilon(\mathbf{k})=v_F|\mathbf{k}|-\mu=x , \tag{3.8}$$

$$\varepsilon(\mathbf{k}-\mathbf{q})=v_F|\mathbf{k}-\mathbf{q}|-\mu=x-q\cos\vartheta , \tag{3.9}$$

having defined

$$q\equiv v_F|\mathbf{q}| . \tag{3.10}$$

The bandwidth E and the chemical potential μ are now given by

$$E=2v_F k_F, \quad \mu=v_F k_F . \tag{3.11}$$

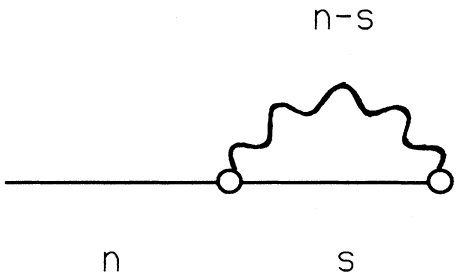

FIG. 4. This diagram corresponds to the standard self-energy to first order. Its specific calculation is performed by keeping ω_D/E_F as a finite parameter instead of considering the usual Migdal limit $\omega_D/E_F\rightarrow 0$.

We begin by reconsidering the calculation of the standard self-energy to first order (Fig. 4). This is not a new diagram, however, the point is that in the usual approach the self-energy is computed in the limit $\omega_D/E_F\rightarrow 0$, while in our case we will keep this ratio as a finite constant.

We use the Green's functions as the Matsubara representations with usual notations.[3] For electrons we have

$$G(i\omega_n,\varepsilon_k)=\frac{1}{i\omega_n-\varepsilon_k-\Sigma(i\omega_n,\mathbf{k})} , \qquad \omega_n=2\pi T[n+\tfrac{1}{2}] \tag{3.12}$$

with chemical potential $\mu=0$, and for phonons

$$D_0(i\omega_n,\omega_0)=\frac{-\omega_0^2}{\omega_m^2+\omega_0^2}, \quad \omega_m=\pi T(2\cdot m) . \tag{3.13}$$

The standard self-energy to first order is given by

$$\Sigma(i\omega_n)=-Tg^2\sum_{\mathbf{k}_s}\sum_{s} G_0(i\omega_s,\varepsilon_{k_s})D_0(i\omega_n-i\omega_s,\omega_0)$$

$$=-Tg^2N_0\sum_{s}\int_{-E/2}^{E/2}dx\frac{1}{i\omega_s-x}\frac{-\omega_0^2}{(\omega_n-\omega_s)^2+\omega_0^2} . \tag{3.14}$$

Considering that

$$\int_{-E/2}^{E/2}dx\frac{1}{i\omega_s-x}=\int_{-E/2}^{E/2}dx\frac{-(i\omega_s+x)}{\omega_s^2+x^2}$$

$$=-i2\arctan\left[\frac{E}{2\omega_s}\right] , \tag{3.15}$$

we obtain

$$\Sigma(i\omega_n)=-i\omega_n\lambda T\sum_{s>0}\arctan\left[\frac{E}{2\omega_s}\right]\frac{8\omega_0^2\omega_s}{[(\omega_s-\omega_n)^2+\omega_0^2][(\omega_s+\omega_n)^2+\omega_0^2]} . \tag{3.16}$$

The wave-function renormalization is given by

$$Z(i\omega_n)=1-\frac{1}{i\omega_n}\Sigma(i\omega_n) . \tag{3.17}$$

Considering the case $\omega_n=0$ and neglecting the temperature dependence ($T\to 0$)

$$T\sum_s \to \frac{1}{2\pi}\int_{-\infty}^{+\infty} d\omega \tag{3.18}$$

we obtain

$$Z=1+\frac{\lambda}{2\pi}\int_0^{\infty} d\omega \arctan\left[\frac{E}{2\omega}\right]\frac{8\omega_0^2\omega}{(\omega^2+\omega_0^2)^2} . \tag{3.19}$$

Introducing

$$y=\frac{\omega}{\omega_0},\quad m=\frac{2\omega_0}{E}=\frac{\omega_0}{E_F} \tag{3.20}$$

and integrating by parts we have

$$Z=1+\lambda\frac{4}{\pi}\int_0^{\infty} dy \frac{m}{1+m^2y^2}\frac{1}{2}\frac{y^2}{y^2+1} . \tag{3.21}$$

The integrand has poles at $y=\pm i$ and $y=\pm i/m$. Considering the contour in the upper half-plane we finally arrive at the expression

$$Z(m)=1+\lambda\left[\frac{1}{1+m}\right] . \tag{3.22}$$

In the usual case $m\to 0$ and we recover the standard expression $Z=1+\lambda$. For a finite value of m however we have a correction factor as given by Eq. (3.22). Therefore, the fact that ω_0/E is different from zero reduces the wave-function renormalization due to the standard self-energy. In view of the discussion of the previous section we can see that this reduction corresponds to an enhancement of T_c. In order to avoid confusion we define m as the nonadiabatic parameter and $m\to 0$ is the adiabatic limit. In this case one has the standard superconductivity that is still a nonadiabatic phenomenon but here we use the terms "adiabatic" and "nonadiabatic" in relation to the nature of the electron-phonon coupling.

IV. THE VERTEX CORRECTION FUNCTION

In this section we will compute the vertex correction function[16] corresponding to the diagram of Fig. 5. As we are going to see this function can be positive and negative and it is strongly dependent on the frequency and momentum of the exchanged phonon (q,ω). We use the model and the schematizations discussed in the previous section. Since the model has no well-defined Brillouin zone we assume for the maximum momentum $q_{\max}=E$, however, its precise maximum value can only be specified within a realistic model. This is actually a very important point because for small values of q the vertex function is positive while it is negative for large values of q. Therefore a modulation in the coupling $g_{k,q}$ or a cutoff due to other reasons are crucial elements to enhance or reduce the value of the critical temperature. We will come back on this point in the discussion and in paper II. It is useful to introduce a dimensionless momentum

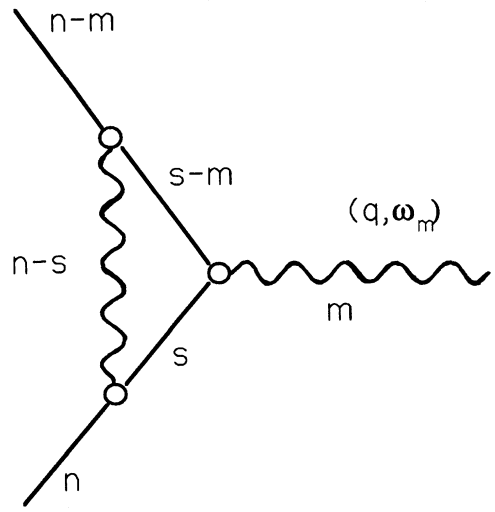

FIG. 5. First-order vertex correction diagram. The resulting vertex correction function can be positive or negative depending on the values of the momentum (q) and frequency (ω_m) of the emitted phonon.

$$Q=\frac{q}{E},\quad Q_{\max}=1 . \tag{4.1}$$

For the moment we consider the case $\omega_n=0$. This is an external variable and the characteristic behavior of the ω_n dependence in the gap equation is defined by a cutoff that will be present anyhow in this equation. So it should not be particularly important to consider the explicit ω_n dependence. Later we will consider this dependence explicitly to show that indeed it is not crucial.

The vertex function that multiplies the bare vertex to include the first correction beyond Migdal is

$$\Lambda(\omega_m,q;\omega_0,E)=1+\lambda P_V(\omega_m,q;\omega_0,E)$$
$$=1-g^2T\sum_{\omega_s}\sum_{\mathbf{k}_s}\left[\frac{1}{i\omega_s-\varepsilon(\mathbf{k}_s)}\right]\left[\frac{-\omega_0^2}{(\omega_n-\omega_s)^2+\omega_0^2}\right]\left[\frac{1}{i(\omega_s-\omega_m)-\varepsilon(\mathbf{k}_s-\bar{q})}\right] , \tag{4.2}$$

where the vertex correction function P_v is a function of the phonon variables ω_m and q and it depends parametrically on ω_0 and $E=2E_F$. In addition we neglect the temperature dependence associated with the variable ω_s and consider the $T\to 0$ limit [Eq. (3.18)]. Using also the approximation of Eq. (3.3) we have

$$P_V(\omega_m,q;\omega_0,E)=\frac{1}{2\pi}\int_{-E/2}^{E/2} dx\int_{-\infty}^{+\infty} d\omega\frac{1}{2}\int_{-1}^{1} d\eta\frac{1}{i\omega-x}\frac{\omega_0^2}{\omega^2+\omega_0^2}\frac{1}{[i(\omega-\omega_m)-(x-q\cdot\eta)]} . \tag{4.3}$$

In this equation we have introduced the angular dependence as a correction factor to the angular independent case. In

three dimensions the angular averaging for a function $f(\vartheta)$ of the scattering angle θ ($\eta=\cos\theta$) is given by

$$\frac{\int_0^{\pi} f(\theta)2\pi\sin\vartheta\, d\vartheta}{\int_0^{\pi} 2\pi\sin\vartheta\, d\vartheta}=\frac{1}{2}\int_{-1}^{1} f(\eta)d\eta\ . \tag{4.4}$$

In view of the strong dependence on momentum that we will obtain for P_V this is a point to reconsider in view of the application of our results to systems with reduced dimensionality.

We are going to integrate first in ω so it is convenient to rewrite P_V as

$$P_V=-\frac{1}{EQ}\frac{1}{2\pi}\int_{-E/2}^{E/2}dx\int_{-\infty}^{+\infty}d\omega\frac{1}{2}\int_{-EQ}^{EQ}dy\frac{1}{(\omega+ix)[\omega-\omega_m+i(x-y)]}\frac{\omega_0^2}{(\omega+i\omega_0)(\omega-i\omega_0)}\ , \tag{4.5}$$

in which we have used the new variables $y=q$, η, and Eq. (4.1). In order to perform the ω integration it is convenient to split the integrand as the sum of relatively simple terms:

$$\begin{aligned}P_V=\frac{1}{EQ}\frac{1}{i}\int_{-E/2}^{E/2}dx\frac{1}{2}\int_{-EQ}^{EQ}dy\frac{\omega_0}{2(\omega_m+iy)}\frac{1}{2\pi}\\ \times\int_{-\infty}^{+\infty}d\omega\left[\frac{1}{\omega-i\omega_0}\frac{1}{\omega+ix}-\frac{1}{\omega+i\omega_0}\frac{1}{\omega+ix}-\frac{1}{\omega-i\omega_0}\frac{1}{[\omega-\omega_m+i(x-y)]}\right.\\ \left.+\frac{1}{\omega+i\omega_0}\frac{1}{[\omega-\omega_m+i(x-y)]}\right]\ .\end{aligned} \tag{4.6}$$

Consider the first term in the ω integration. If $x<0$ both singularities are in the upper half-plane, so one could close the contour in the lower half-plane and the integral would give zero. This leads to [see Fig. 6(a)]

$$I_1=\frac{1}{2\pi}2\pi i\frac{\vartheta(x)}{i\omega_0+ix}=\frac{\vartheta(x)}{\omega_0+x}\ . \tag{4.7}$$

The second term gives [see Fig. 6(b)]

$$I_2=-\frac{-1}{2\pi}2\pi i\frac{\vartheta(-x)}{-i\omega_0+ix}=\frac{-\vartheta(-x)}{\omega_0-x}\ . \tag{4.8}$$

The two terms given by Eqs. (4.7) and (4.8) will cancel when integrating over x so we can neglect them. The other two terms give [see Figs. 6(c) and 6(d)]

$$I_3=-\frac{1}{2\pi}(2\pi i)\frac{\vartheta(x-y)}{i\omega_0-\omega_m+i(x-y)}=-\frac{\vartheta(x-y)}{\omega_0+i\omega_m+(x-y)}\ . \tag{4.9}$$

$$I_4=\frac{1}{2\pi}(-2\pi i)\frac{\vartheta(y-x)}{-i\omega_0-\omega_m+i(x-y)}=\frac{\vartheta(y-x)}{\omega_0-i\omega_m-(x-y)}\ . \tag{4.10}$$

From Eq. (4.6), (4.9), and (4.10) we obtain

$$P_V=\frac{1}{EQ}\int_{-E/2}^{E/2}dx\frac{1}{2}\int_{-EQ}^{EQ}dy\frac{\omega_0}{2i}\frac{1}{\omega_m+iy}\left[\frac{-\vartheta(x-y)}{\omega_0+i\omega_m+(x-y)}+\frac{\vartheta(y-x)}{\omega_0-i\omega_m-(x-y)}\right]\ . \tag{4.11}$$

Considering that

$$\int_{-x_0}^{x_0}dx\int_{-y_0}^{y_0}dy\,\vartheta(y-x)f(x,y)=\int_{-x_0}^{x_0}dx\int_{-y_0}^{y_0}dy\,\vartheta(x-y)f(-x,-y)\ , \tag{4.12}$$

we can rewrite Eq. (4.11) for relatively small values of y, ($y<E/2$) as

$$P_V=\frac{\omega_0}{EQ}\frac{1}{2}\int_{-EQ}^{EQ}dy\int_{y}^{E/2}dx\frac{\omega_m^2+y[\omega_0+(x-y)]}{(x_m^2+y^2)\{[\omega_0+(x-y)]^2+\omega_m^2\}}\ . \tag{4.13}$$

Introducing the new variables

$$\begin{aligned}u&\equiv x-y\ ,\\ z&\equiv u+\omega_0\ ,\end{aligned} \tag{4.14}$$

we have

$$P_V=\frac{\omega_0}{EQ}\frac{1}{2}\int_{-EQ}^{EQ}dy\int_{\omega_0}^{E/2-y+\omega_0}\frac{\omega_m^2+y\cdot z}{(\omega_m^2+y^2)(z^2+\omega_m^2)}dz\ . \tag{4.15}$$

Considering the z integration, the first term in Eq. (4.15) gives

$$\int_{\omega_0}^{E/2-y+\omega_0}dz\frac{1}{\omega_m^2+z^2}=\frac{1}{\omega_m}\left[\arctan\frac{\omega_m}{\omega_0}-\arctan\frac{\omega_m}{E/2+\omega_0-y}\right] \tag{4.16}$$

and the second term is

$$\int_{\omega_0}^{E/2-y+\omega_0}\frac{z}{z^2+\omega_m^2}dz=\frac{1}{2}\ln\left[\frac{\omega_m^2+(E/2-y+\omega_0)^2}{\omega_0^2+\omega_m^2}\right]\ . \tag{4.17}$$

Inserting Eqs. (4.16) and (4.17) into Eq. (4.15) leads to

$$P_V=\frac{\omega_0}{EQ}\frac{1}{2}\int_{-EQ}^{EQ}dy\frac{1}{\omega_m^2+y^2}\left\{\omega_m\left[\arctan\frac{\omega_m}{\omega_0}-\arctan\frac{\omega_m}{E/2+\omega_0-y}\right]+\frac{y}{2}\ln\left[\frac{\omega_m^2+(E/2-y+\omega_0)^2}{\omega_0^2+\omega_m^2}\right]\right\}\ . \tag{4.18}$$

In order to proceed with the y integration it is convenient to expand the term in the curly brackets $\{\cdots\}$ for small values of y. This is consistent with the fact that our initial schematizations [Eqs. (3.7) and (3.8)] are also consistent with small values of Q and therefore of y. We will expand up to quadratic terms in y so that for the ln term we only consider the linear term because this is multiplied by y. This is

$$\ln\frac{(E/2+\omega_0-y)^2+\omega_m^2}{\omega_0^2+\omega_m^2}\cong\ln\left[\frac{(E/2+\omega_0)^2+\omega_m^2}{\omega_0^2+\omega_m^2}\right]-\frac{2(E/2+\omega_0)}{(E/2+\omega)^2+\omega_m^2}y\ . \tag{4.19}$$

For the other two terms we can consider that

$$\frac{d}{dy}\arctan f(y)=\frac{1}{1+f^2}f'\qquad\left[f'=\frac{df}{dy}\right]\ , \tag{4.20}$$

$$\frac{d^2}{dy^2}\arctan f(y)=\frac{1}{1+f^2}\left[f''-\frac{2f\cdot f'^2}{1+f^2}\right]\ . \tag{4.21}$$

Since in our case

$$f(y)=\frac{\omega_m}{E/2+\omega_0-y}\ , \tag{4.22}$$

$$f'|_{y=0}=\frac{\omega_m}{(E/2+\omega_0)^2}\ , \tag{4.23}$$

$$f''|_{y=0}=\frac{2\omega_m}{(E/2+\omega_0)^3}\ , \tag{4.24}$$

and considering that in Eq. (4.18) only the quadratic term in y will lead to a nonzero contribution we have

$$\begin{aligned}\frac{1}{2}\frac{d^2}{dy^2}\arctan f(y)\Big|_{y=0}&=\frac{\frac{1}{2}(E/2+\omega_0)^2}{(E/2+\omega_0)^2+\omega_m^2}\\&\times\left\{\frac{2\omega_m}{(E/2+\omega_0)^3}-\frac{2\omega_m}{E/2+\omega_0}\frac{\omega_m^2}{(E/2+\omega_0)^2}\frac{1}{(E/2+\omega_0)^2+\omega_m^2}\right\}\\&=\frac{\omega_m(E/2+\omega_0)}{[(E/2+\omega_0)^2+\omega_m^2]^2}\ .\end{aligned} \tag{4.25}$$

The result of this expansion in Eq. (4.18) gives therefore

$$P_V=\frac{\omega_0}{EQ}\left[\int_0^{EQ}\frac{A}{(\omega_m^2+y^2)}dy+\int_0^{EQ}\frac{By^2}{(\omega_m^2+y^2)}dy\right] \tag{4.26}$$

having introduced

$$A=\omega_m\left[\arctan\left[\frac{\omega_m}{\omega_0}\right]-\arctan\frac{\omega_m}{(E/2+\omega_0)}\right]\ , \tag{4.27}$$

$$B=-\frac{(E/2+\omega_0)[(E/2+\omega_0)^2+2\omega_m^2]}{[(E/2+\omega_0)^2+\omega_m^2]^2} . \tag{4.28}$$

The y integrations can now be performed to arrive at our final result that is the central point of this paper:

$$P_V(\omega_m,Q;\omega_0,E)=\frac{\omega_0}{EQ}\left[\left[\arctan\frac{\omega_m}{\omega_0}-\arctan\frac{\omega_m}{E/2+\omega_0}\right]\arctan\left[\frac{EQ}{\omega_m}\right]\right.$$
$$\left.-\left[EQ-\omega_m\arctan\frac{EQ}{\omega_m}\right]\frac{(E/2+\omega_0)[(E/2+\omega_0)^2+2\omega_m^2]}{[(E/2+\omega_0)^2+\omega_m^2]^2}\right] . \tag{4.29}$$

This result is pure real while in general one may expect that the vertex correction function should be complex. However, in our schematization of half-filled bands combined with a small-q expansion, the imaginary part vanishes exactly.

In order to clarify the dependence on ω_m and Q it is useful to consider the following limits. The *static limit* corresponds to taking first the limit $\omega_m\to 0$ and then the limit $Q\to 0$. In this case we have

$$\lim_{Q\to 0}\lim_{\omega_m\to 0}P_V(\omega_m,Q;\omega_0,E)=-\frac{\omega_0}{E/2+\omega_0} . \tag{4.30}$$

The vertex function is negative in this limit and this result is in agreement with the calculation of Grabowsky and Sham[18] who only considered this limit in the context of plasmons and from this argued that vertex corrections should be negative in general. We can see that this is not the case and, in fact, if we reverse the order of the two limits we obtain the *dynamical limit* that is positive

$$\lim_{Q\to 0}P_V(\omega_m,Q;\omega_0,E)=\frac{\omega_0}{\omega_m}\left\{\arctan\frac{\omega_m}{\omega_0}-\arctan\frac{\omega_m}{E/2+\omega_0}\right\} \tag{4.31}$$

and

$$\lim_{\omega_m\to 0}\lim_{Q\to 0}P_V(\omega_m,Q;\omega_0,E)=\frac{E/2}{E/2+\omega_0} . \tag{4.32}$$

The sign of the function P_V is represented in Fig. 7 by the open areas in the plane (Q,ω_m) for two different values of ω_0/E_F (note that $E=2E_F$). It results that small values of Q correspond mainly to positive vertex corrections. The behavior of $P_V(\omega_m)$ for different values of Q and $\omega_0/E_F=1$ is shown in Fig. 8.

In order to estimate the average effect of the vertex correction function P_V we can take an average over frequencies and momenta. In doing this one should consider that, since P_V depends strongly on Q and our model calculation is highly idealized, a specific physical mechanism or a more realistic model may introduce a modulation of the scattering as a function of Q and eventually

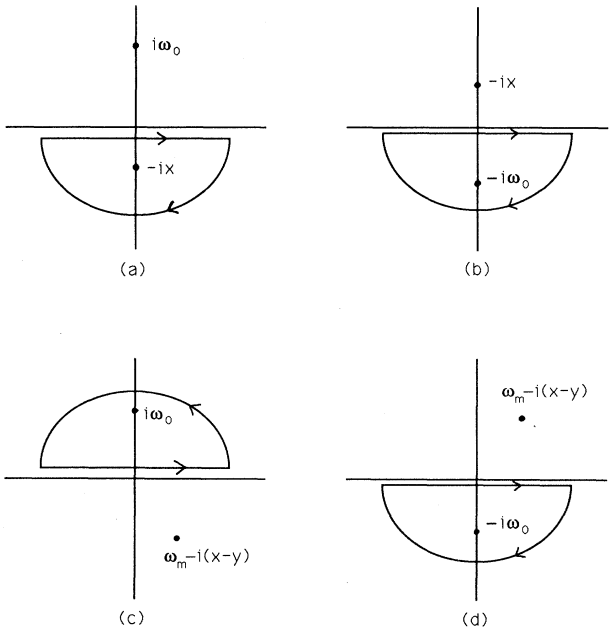

FIG. 6. Poles and contours of integration in ω for the various terms in Eq. (4.6).

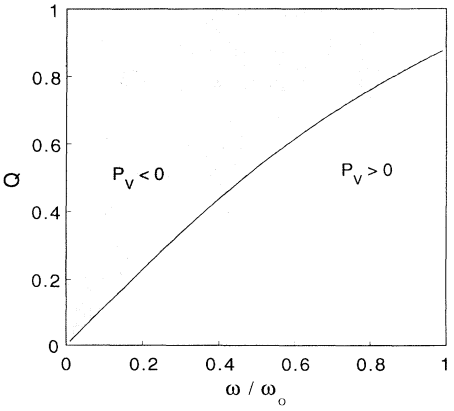

FIG. 7. We report in this figure the sign of the vertex function $P_V(\omega,Q)$ for $\omega_0/F_E=1.0$. The open areas correspond to $P_V>0$ and the dark areas to $P_V<0$. From the behavior of the function $P_V(\omega,Q)$ it results that the limit case $P_V(0,0)$ depends crucially on the order of the limits. The structure of $P_V(\omega,Q)$ is therefore rather complex and its is nontrivial to extrapolate its full role in the gap equation by considering only limiting cases.

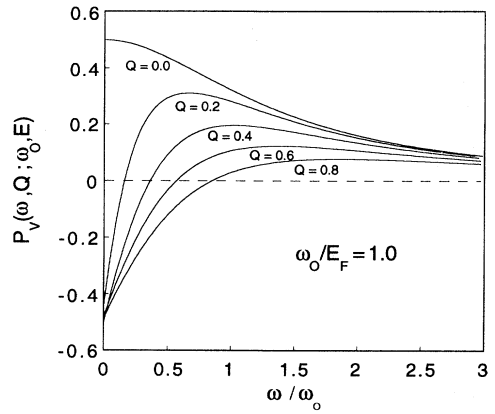

FIG. 8. Behavior of $P_V(\omega)$ for different values of Q. For small Q values the positive part of the vertex function becomes predominant.

also of ω_m. For this reasons we introduce a cutoff Q_c for the average over momenta and consider how the average of the vertex function depends on Q_c itself. For the frequency average a natural cutoff is automatically provided by ω_0 so it is not necessary to consider further limitations. In Fig. 9, the solid lines represent the average values of P_V corresponding to different values of Q_c as a function of the Migdal parameter ω_0/E_F. In the Migdal limit ($\omega_0/E_F \to 0$) the whole effect vanishes and one recovers Migdal's theorem. However for finite values of ω_0/E_F the effect is quite appreciable and it depends strongly on the value of Q_c and therefore on the range of

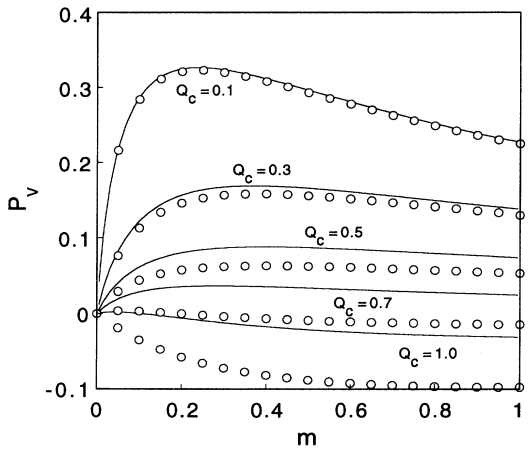

FIG. 9. In order to estimate the total effect of the vertex function $P_V(Q,\omega)$ (solid lines) on the gap equation it useful to consider its average with respect to Q and ω as a function of $m = \omega_0/E_F$. While for ω a natural cutoff is provided by ω_0, for the average over Q specific modulations may be introduced by specific models. For this reason we have considered different cutoff values Q_c. The result is that small values of Q_c correspond to globally positive vertex correction. We have also tested the validity of our analytical scheme by including explicitly the q^2 terms [Eq. (3.6)] and performing a numerical analysis that corresponds here to the little circles.

momenta that are relevant for the system in question.

In order to check the validity of our approximation to neglect the terms of order q^2 in Eq. (3.6) we have included these terms and computed the average function P_V numerically. The results of this calculation are represented by small squares in Fig. 9 and they give an idea of the validity of our analytical scheme. Clearly it is very good for small values of Q while for large values of Q the deviation from the numerical results become appreciable.

In order to proceed systematically in a diagrammatic expansion an important clue is provided by the Ward identities that relate vertex corrections to the self-energy. In our case a Ward identity can be written in the following way:

$$Z(i\omega_n = 0) = \lim_{\omega_m \to 0} \lim_{Q \to 0} P_V(\omega_m, Q; \omega_0, E)$$
$$= 1 + \lambda \left[\frac{1}{1+m} \right] . \tag{4.33}$$

This Ward identity refers to the propagation of a single electron and it seems to support the simple argument of Sec. II about the order of the various diagrams. In paper II however we are going to see that for superconductivity the situation is more complex because one should refer to the pair of interacting electrons. The correct Ward identity for superconductivity will imply a (small) correction with respect to Eq. (4.33).

Up to now we have only considered the case $\omega_n = 0$ in Fig. 5. This was because an eventual structure of P_V with respect to ω_n would not have much effect once inserted in the gap equation. However we have also considered the case $\omega_n \neq 0$ explicitly. Defining $\omega_1 = \omega_m$ and $\omega_2 = \omega_n - \omega_m$ in Fig. 10(a) we show the sign of the function P_V for $Q = 1.0$ and $\omega_0/E_F = 1.0$. The open areas correspond to $P_V > 0$. In Fig. 10(b) we show the same plot for $Q = 0.1$. The comparison with Fig. 10(a) shows again that small values of Q enhance the areas of positive values for P_V.

In summary the main result of this section is provided by Eq. (4.29) that shows a complex behavior of the vertex function P_V on the momentum and frequency of the exchanged phonon. Even its sign depends crucially on these parameters as shown in Fig. 7. This situation is therefore quite different from the previous simplified studies of the vertex corrections that did not include these dependencies.[18–21] Our analytical expression [Eq. (4.29)] is derived using various schematizations some of which we have tested by a numerical analysis that has confirmed the general behavior of the analytical result. Our starting model is extremely simplified and, in the same sense, it can be related to the properties of the free-electron gas. It is important therefore to consider the properties of real systems for which various other effects have to be included. Apart from the obvious effects of the specific Brillouin zone and band structure a general element that appears to be characteristic of all high-T_c superconductors is the important role of the electronic correlations due to Coulomb interactions. In the next section we are going to discuss in a simple way the role of these correlations with respect to the vertex functions.

V. ELECTRONIC CORRELATIONS AND REAL MATERIALS

The calculation of the vertex function in Sec. IV refers to a highly simplified model that, in some sense, can be considered as the free-electron gas. Despite this simplicity the result shows a complex structure with respect to frequency and momentum. Therefore its application to real systems is a delicate matter. Here we are going to present some considerations about the effects of a more realistic picture on the vertex corrections.

Clearly one should consider the full band structure of the system in the calculation. One can expect that many specific details of the band structure will not modify appreciably the main features of the vertex function in view of the averaging procedures on which it is based. However strong peaks in the density of state[20] (DOS) may be relevant for the dependence on q and ω of the vertex function. For example, if the Fermi level lies near a peak of the DOS, small-q scattering acquires a larger weight with respect to large-q scattering because it involves regions of the Fermi surface corresponding to larger values of the DOS. Large-q scattering instead will be independent on the starting point and it will sample the average value of the DOS on the whole Brillouin zone. This situation would enhance the positive regions of the vertex functions. The opposite would happen instead if the Fermi level is located near a minimum of the DOS. It is also interesting to compare our results with the vertex corrections obtained in the limit of unfinite dimension.[34] Clearly in this limit one loses the strong q dependence of the nonadiabatic terms, however, the band filling can also give rise to important effects that appear to lead to positive corrections in the case of relatively few carriers.[35] In this respect our calculations refer only to the half-filled case but it should be possible to generalize them to other situations.

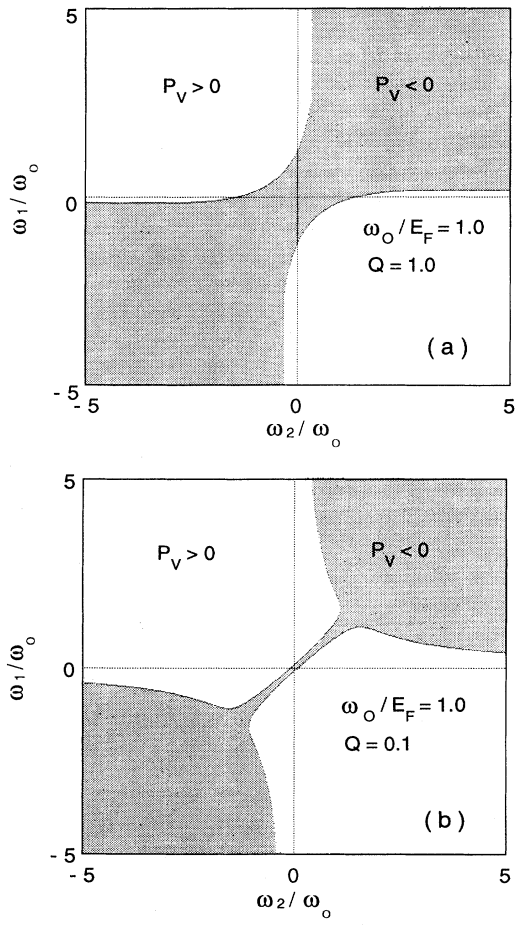

FIG. 10. Generalization of the vertex function to the case $\omega_n \neq 0$ (Fig. 5). Defining $\omega_1=\omega_n$ and $\omega_2=\omega_n-\omega_m$ (Fig. 5) we show the sign of the function P_V in the map of ω_1,ω_2 for $Q=1.0$. The open regions correspond to $P_V>0$. (b) Same plot for $Q=0.1$. Also, in this more general case small values of Q favor positive vertex corrections.

Apart from the specific band-structure effects a crucial element common to all high-T_c superconductors is the role of electronic correlations induced by Coulomb interactions.[8,9,22] In fact, even if our starting point of view is that of a Fermi liquid, many properties of these systems, like the phase diagram for the oxides[8,9] and the band filling for the Fullerene compounds,[11] can only be understood with Hubbard-type models. This implies that even in the case of metallic properties, those that are associated with superconductivity, electronic correlations are expected to play an important role. It is important therefore to include these properties in the structure of our vertex function. One effect is a renormalization of the parameters, however, more important is the possible modulation of the electron-phonon coupling g as a function of q and ω.

For example, in a simple jellium model[23] the screened electron-electron potential $V(q,\omega)$ is

$$V(q,\omega)=\frac{4\pi e^2}{q^2+k_s^2}\frac{\omega^2}{\omega^2-\omega^2(q)}\ , \tag{5.1}$$

where k_s is the Thomas-Fermi wave vector and $\omega(q)$ is the phonon spectrum. For $\omega<\omega(q)$ the interaction becomes attractive and the amplitude is larger for small values of q with an upper cutoff at k_s. The value of k_s can be estimated from

$$k_s^2=\frac{4\pi e^2}{\varepsilon_\infty}N(0)\ , \tag{5.2}$$

where ε_∞ refers to the atomic or ionic polarizability, that in a more realistic picture is given by the interband transitions. $N(0)$ is the DOS at the Fermi level. High-T_c materials are in some sense closer to doped ionic systems than to normal metals.[23] This implies that ε_∞ can be rather larger but the metallic part of the screening, and therefore k_s, is expected to be rather small. This implies that small momentum scattering is predominant and gives more weight to the positive regions of $P_V(q,\omega)$.

The above jellium model is not very realistic for fullerene and cuprate compounds that are usually described in terms of a tight-binding picture. For example, in fullerene compounds it is believed that the main electron-phonon coupling is the one with the vibrations of a single molecule.[13] This would lead to a picture as shown in Fig.

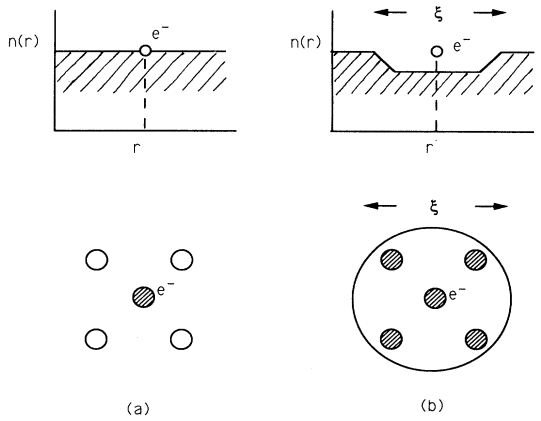

FIG. 11. Schematic picture of the electron-phonon interaction for uncorrelated (a) and correlated (b) electron. In the first case an electron does not perturb the electronic density $n(r)$ and it interacts with the vibrations of a single molecule (shaded). In case of correlation (b) an electron is accompanied by a correlation hole of size ξ and it will interact with all the molecules within this zone.

11 in which an electron at position r interacts only with one molecule and, if one neglects correlations, it does not perturb the average electronic density $n(r)$. This corresponds to the simple Hamiltonian

$$H=\sum_i g_0 c_i^\dagger c_i \phi_i \ , \tag{5.3}$$

where the index i refers to the position of the molecules and ϕ_i is the phonon field at r_i. Due to the local nature of the interaction the resulting $g(q)=g_0$ is structureless. However if we consider that electrons are actually correlated we should associate to each electron the corresponding correlation hole of size ξ [Fig. 11(b)]. This implies that a perturbation of the electron density at position r will interact with all the molecular vibrations within the size of the correlation hole ξ. This leads to a generalization of Eq. (5.3) into

$$H=\sum_i c_i^\dagger c_i \sum_j g_0 \phi_j f(|i-j|) \ , \tag{5.4}$$

where the function $f(|i-j|)$ describes the delocalization of the interaction. In the limit of no correlations $f(|i-j|)=\delta_{ij}$ and one recovers Eq. (5.3). If, on the other hand, this function extends over a zone of size ξ, the resulting electron-phonon coupling in q space will acquire a structure factor $f(q)$ that is the Fourier transform of $f(|i-j|)$

$$g(q)=g_0 \cdot f(q) \ . \tag{5.5}$$

This structure factor will be characterized by an upper cutoff q_c of the order

$$q_c \cong \xi^{-1} \ . \tag{5.6}$$

Therefore we see that also in the case of a tight-binding picture it is reasonable to expect an upper cutoff over the scattered momenta due to electronic correlations. In a highly simplified picture ξ^{-1} can also be related to k_s, however a more detailed study seems to be necessary. Recently a step in this direction has been made by Kulic and Zeyher and by Grilli and Castellani[24] who have computed in various ways the effect of strong electronic correlations on the electron-phonon interaction. Their results qualitatively confirm our simplified discussion and provide a systematic scheme to describe these effects. In particular Kulic and Zeyher present a detailed study of $g(q)$ as a function of doping. The result is that, for small doping, $g(q)$ is enhanced for small-q values and decays rapidly beyond a characteristic value q_c that is strongly dependent on the doping. An interesting property is that the average value of the resulting λ is about constant for different values of the doping. This situation seems to support therefore one specific choice for the structure of $g(q)$ that we are going to discuss in paper II.

We can conclude therefore that, in general, electronic correlations introduce a structure in $g(q)$ with an upper cutoff for the momenta. Considering the structure of the vertex function (Sec. IV), whose sign is shown in Fig. 7, this upper cutoff will unbalance the situation in favor of the positive part of the vertex function.

Another effect of the Coulomb interaction in relation to superconductivity is provided by the so-called pseudopotential term μ^*.[25,26] This term is constructed by the static screened repulsion μ corrected by the dynamic effects of the retarded interaction. Usually this term is included in the gap equation and described in terms of the electron gas. In the high-T_c SC the situation is more complex because one has a large static screening due to interband transitions and a relatively small metallic screening in view of the low carrier density. In such a situation the usual description is rather unrealistic.

The most accurate analysis of μ^* for the fullerene compounds (that however also involves drastic simplifications) is due to Gunnarson and the result is $\mu^* \simeq 0.4$.[26] This value is much larger than the usual one for normal superconductors ($\mu^* \simeq 0.1$) and it makes it difficult to interpret the data of the fullerene compounds (Table I) by means of the usual Migdal-Eliashberg theory (see also Sec. II). Given this complex situation we prefer to consider the problem of μ^* separated from the gap equation and to add it at the end. In fact for systems like the high-T_c SC the analysis of μ^* requires one to go beyond the free-electron picture and to add the specific properties of the material.[25] The situation is less critical for the electron-phonon scattering that involves mainly only the states of a single band.

VI. DISCUSSION AND CONCLUSIONS

In this paper we have started a detailed analysis of the implications on superconductivity due to the breakdown of Migdal's theorem. This is a general situation for all the high-T_c superconductors. Our first observation is that it is possible to study this problem in a perturbative scheme with respect to the parameter $\lambda(\omega_D/E_F)$. This of course does not necessarily imply that real materials lie in this regime. However the idea is that the main reasons that may produce an enhancement of T_c should also be valid beyond the perturbative regime.

We have seen that even the standard self-energy acquires a favorable correction factor if evaluated for $\omega_D/E_F \neq 0$. The main part of the paper deals however with a detailed calculation of the vertex function $P_V(q,\omega)$ as a function of momentum and frequency of the exchanged phonon. This function has a nontrivial structure with respect to q and ω and its sign can be positive and negative depending on the region of the (q,ω) plane (Fig. 7). This implies that, depending on the specific properties of the material, the value of T_c can be both enhanced or suppressed by the vertex corrections. In any case this new situation provides a much broader range of possibilities with respect to the usual theory. We have also pointed out how electronic correlations that are certainly relevant in all the high-T_c systems, should favor small q scattering corresponding to positive vertex corrections and to a consequent enhancement of T_c.

We are now in the position of giving a more firm basis to the simplified discussion of Sec. II. A detailed analysis of the generalized gap equation, also including other effects like the cross term that should be kept in a systematic approach, will be presented in paper II. However a simplified scheme within the limits of the present discussion would lead to the following equation for T_c:

$$T_c \cong \omega_0 z_0(\omega_0/E_F)\exp\left\{\frac{-[1+z_0(\omega_0/E_F)\lambda]}{\lambda[1+\langle P_V\rangle\lambda]^2-\mu^*}\right\}, \tag{6.1}$$

where

$$z_0(\omega_0/E_F)=\left[1+\frac{\omega_0}{E_F}\right]^{-1}. \tag{6.2}$$

The prefactor term is due to the integral over available energies restricted to a single band of width $2E_F$. We see that in the Migdal limit $\omega_D/E_F \to 0$ one recovers the usual prefactor ω_0. If however $\omega_D > E_F$ the prefactor becomes essentially equal to E_F and independent on ω_0. This could have important consequences on the isotope effect that can become very small or negligible in view of this effect. The term $z_0(\omega_D/E_F)$ in the numerator of the exponential is due to the reduction of the self-energy effect we have discussed before and it corresponds to an enhancement of T_c independently on q and ω. The vertex correction $\langle P_V\rangle$ corresponds instead to an average over q and ω and it is crucially dependent on the properties of the system in question. Specifically an upper cutoff q_c for the electron-phonon scattering momentum leads to positive values of $\langle P_V\rangle$ as shown in Fig. 9. As we have discussed this cutoff can be provided by electronic correlations. One can also see from Fig. 9 that vertex corrections are appreciable also for relatively small values of the parameter ω_0/E_F. We see therefore that, if positive vertex corrections are dominant, the simple discussion of Sec. II is essentially confirmed by a more detailed analysis.

Concerning the isotope effect, in addition to the prefactor already mentioned we see that the phonon frequency appears also in the terms z_0 and $\langle P_V\rangle$. In the usual approach instead ω_0 appears only in the prefactor and in μ^*. This new situation allows therefore for a more complex structure of the isotope effect in which the exponent α can become very small but also larger than the usual maximum value $\alpha=0.5$. In paper II we are going to proceed more systematically and the corresponding expression for T_c will be more complex. It will confirm however the general trends of the present discussion.

In summary we have presented a study of the consequences of the breakdown of Migdal's theorem on superconductivity. This brings us in a broader situation in which appreciable enhancements of T_c are possible depending on the specific properties of the material. In particular we argue that electronic correlations can represent a possible element to drive the system into a region of parameters that favors positive vertex corrections and therefore enhanced T_c values. This picture is still based on having fermions above T_c, as supported by specific experiments to probe the nature of the transition,[27] however the effects we discuss are the precursors of the polaron picture, however without reaching it. In this respect various experimental data that point to polarons[28] or strong electron-phonon interaction could actually be consistent with the present scheme.

Vertex corrections and other effects beyond Migdal's theorem should of course play an important role in various other properties like transport, the shifts of phonon frequencies,[29] tunneling,[30] and photoemission data.[31] In each of these effects, however, the role of vertex corrections is expected to be different from that played in the superconductivity. It is very important therefore to examine these effects in detail in order to make specific predictions that could be tested by experiments. Finally we would like to mention some work that has been recently performed regarding the nonadiabaticity in the electron-phonon interaction from the point of view of the single molecule in relation with the Jahn-Teller distortions.[32] This work represents a complementary view (local) with respect to our and it would be interesting to consider the possibility of a unifying picture.

ACKNOWLEDGMENTS

It is a pleasure to thank C. Castellani, S. Ciuchi, P. Fulde, M. Grilli, O. Gunnarson, G. Parisi, D. Rainer, G. Sawatzky, and E. Tosatti for interesting discussions. This work was partly supported by a CNR grant.

[1] Y. J. Uemura *et al.*, Phys. Rev. Lett. **66**, 2665 (1991); N. D'Ambrumenil, Nature **352**, 472 (1991).

[2] A. B. Migdal, Sov. Phys. JETP **34**, 996 (1958).

[3] G. Rickayzen, *Green's Functions and Condensed Matter* (Academic, London, 1980).

[4] G. M. Eliashberg, Sov. Phys. JETP **11**, 696 (1960).

[5] P. B. Allen and B. Mitrovic, in *Solid State Physics,* edited by H. Ehrenreich, F. Seitz, and D. Turnbull (Academic, New York, 1982) Vol. 37; J. P. Carbotte, Rev. Mod. Phys. **62**, 1027 (1990); D. J. Scalapino in *Superconductivity* (Ref. 7), Vol. I, p. 449; G. Grimvall, *The Electron-Phonon Interaction in Metals* (North-Holland, Amsterdam, 1981).

[6]W. L. McMillan, Phys. Rev. **167**, 331 (1968).
[7]*Superconductivity,* edited by R. D. Parks (Dekker, New York, 1969).
[8]P. W. Anderson and J. R. Schrieffer, Phys. Today **XX**, 54 (1991).
[9]P. Fulde, Physica C **153-155**, 1769 (1988).
[10]C. Grimaldi, L. Pietronero, and S. Strässler, following paper, Phys. Rev. B **52**, 10 530 (1995).
[11]M. De Seta and F. Evangelisti, Phys. Rev. Lett. **71**, 2477 (1993).
[12]W. E. Pickett, K. Krakaner, R. E. Cohen, and D. J. Singh, Science **255**, 46 (1992); O. K. Andersen *et al.*, Physica C **185-189**, 147 (1991).
[13]W. E. Pickett, in *Solid State Physics,* edited by H. Ehrenreich and F. Spaepan (Academic, New York, 1993).
[14]C. Castellani, C. Di Castro, and W. Metzner, Phys. Rev. Lett. **72**, 316 (1994).
[15]L. Pietronero, Europhys. Lett. **17**, 365 (1992).
[16]L. Pietronero and S. Strässler, Europhys. Lett. **18**, 627 (1992); C. Grimaldi, L. Pietronero, and S. Strässler, Phys. Rev. Lett. **75**, 1158 (1995).
[17]R. Combescot and G. Varelogiannis, Europhys. Lett. **17**, 635 (1992). See also G. Varelogiannis, Ph.D. thesis, Ecole Normale Superieure, Paris, 1993; P. Benedetti, C. Grimaldi, L. Pietronero, and G. Varelogiannis, Europhys. Lett. **28**, 351 (1994).
[18]M. Grabowsky and L. J. Sham, Phys. Rev. B **29**, 6132 (1984).
[19]J. Cai, X. L. Lei, and L. M. Xie, Phys. Rev. B **39**, 11 618 (1989).
[20]H. R. Krishnamurthy, D. M. Newns, P. C. Pattnaik, C. C. Tsuei, and C. C. Chi, Phys. Rev. B **49**, 3520 (1994).
[21]V. N. Kostur and B. Mitrovic, Phys. Rev. B **48**, 16 388 (1993).
[22]R. W. Lof, M. A. van Veenendall, B. Koopmans, H. T. Jonkman, and G. Sawatzky, Phys. Rev. Lett. **68**, 3924 (1992).
[23]A. A. Abrikosov, Physica C **222**, 191 (1994).
[24]M. L. Kulic and R. Zeyher, Phys. Rev. B **49**, 4395 (1994); Physica B **199&200**, 358 (1994); M. Grilli and C. Castellani, Phys. Rev. B **50**, 16 880 (1994).
[25]J. H. Kim and Z. Tesanovic, Phys. Rev. Lett. **71**, 4218 (1993).
[26]O. Gunnarson and G. Zwicknagl, Phys. Rev. Lett. **69**, 957 (1992).
[27]D. van der Marel and G. Rietveld, Phys. Rev. Lett. **69**, 2575 (1992); G. Rietveld, N. Y. Chen, and D. van der Marel, *ibid.* **69**, 2578 (1992).
[28]A. S. Alexandrov and N. F. Mott, Supercond. Sci. Technol. **6**, 215 (1993).
[29]R. Zeyher and G. Zwicknagl, Z. Phys. B **78**, 175 (1990).
[30]D. Rainer (unpublished).
[31]O. Gunnarson, V. Meden, and K. Schönhammer (unpublished).
[32]A. Auerbach, N. Mainini, and E. Tosatti, Phys. Rev. B **49**, 12 998 (1994); **49**, 13 008 (1994).
[33]M. S. Dresselhaus and G. Dresselhaus, Adv. Phys. **30**, 139 (1981).
[34]S. Ciuchi (unpublished).
[35]J. K. Freericks, Phys. Rev. B **50**, 403 (1994).

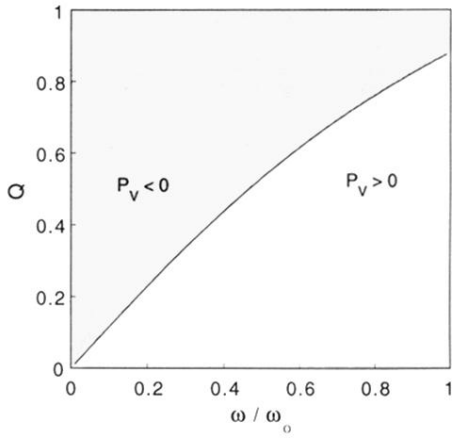

FIG. 7. We report in this figure the sign of the vertex function $P_V(\omega,Q)$ for $\omega_0/F_E=1.0$. The open areas correspond to $P_V>0$ and the dark areas to $P_V<0$. From the behavior of the function $P_V(\omega,Q)$ it results that the limit case $P_V(0,0)$ depends crucially on the order of the limits. The structure of $P_V(\omega,Q)$ is therefore rather complex and its is nontrivial to extrapolate its full role in the gap equation by considering only limiting cases.